BIOLOGY OF REPRODUCTION (2012) **86**(2):44, 1–9
Published online before print 19 October 2011.
DOI 10.1095/biolreprod.111.093229

Changes of Large Molecular Weight Hyaluronan and Versican in the Mouse Pubic Symphysis Through Pregnancy[1]

Renata Giardini Rosa,[3,4] Yucel Akgul,[3] Paulo Pinto Joazeiro,[4] and Mala Mahendroo[2,3]

[3]*Department of Obstetrics and Gynecology and The Cecil H. and Ida Green Center for Reproductive Biology Sciences, University of Texas Southwestern Medical Center, Dallas, Texas*
[4]*Department of Histology and Embryology, Institute of Biology, State University of Campinas (UNICAMP), Campinas, Sao Paulo, Brazil*

ABSTRACT

During pregnancy, the mouse pubic symphysis undergoes expansion and remodeling resulting in formation of a flexible and elastic interpubic ligament allowing passage of a term fetus. In the current study, we sought to identify and characterize components of the extracellular matrix that likely play an important role in elongation and flexibility of the interpubic ligament during parturition. Mouse pubic symphyses and interpubic ligaments collected at time points during pregnancy and postpartum were utilized to evaluate collagen type, collagen content, processing and solubility, matricellular protein, and proteoglycan expression and quantitative assessment of all glycosaminoglycans. These studies revealed increased gene expression for hyaluronan synthase 1, hyaluronan synthase 2, and versican on Gestation Day 18 as well as a decline in protein expression for the versican-degrading protease a disintegrin-like and metalloprotease with thrombospondin type 1 (ADAMTS1) motif. These findings suggest that the primary mediators of increased elongation and flexibility of the interpubic ligament at term result from increased synthesis and reduced metabolism of viscoelasticity-promoting molecules such as high molecular weight hyaluronan and versican.

collagen, extracellular matrix, hyaluronan, mouse, pregnancy, pubic symphysis

INTRODUCTION

During pregnancy, the pubic symphysis (PS) undergoes finely tuned hormonally regulated remodeling to allow the pubic bones to separate and accommodate safe passage of the fetus through the birth canal. The remodeling of the cartilaginous PS is a stepwise process involving reabsorption of bone and conversion of cartilage to a flexible interpubic ligament (IpL). Formation of the IpL occurs in numerous species including mouse and guinea pig [1–3]. While it has not been well studied in the human, there is evidence that PS remodeling occurs during pregnancy [4–6]. In mice, this process begins on the 10th day of a 19-day pregnancy. This modification involves gradual expansion of the dense connective tissue as well as dedifferentiation of chondrocytes to form fibroblasts. These fibroblasts proliferate to produce a symphyseal structure that resembles a true ligament [7]. By Gestation Day (d) 14, the ligament is fully formed. The interpubic ligament fibroblasts secrete numerous extracellular matrix (ECM) components and are proposed to acquire a myofibroblast phenotype at the end of pregnancy, as determined by ultrastructural and immunohistochemistry analyses [8]. Following labor, the ligament undergoes rapid involution, and within 3–5 days postpartum (pp), the PS is remodeled to its original size, with similar morphology [9].

The transformation of the pubic symphysis to an IpL during pregnancy is regulated in part by the peptide hormone relaxin as well as by estrogen. Relaxin is a pleiotropic hormone with diverse functions in both reproductive and nonreproductive tissues, such as promoting matrix remodeling, cell proliferation, inhibition of tissue fibrosis, and apoptosis. Its importance in progressive growth and remodeling of the cervix, vagina, and PS was first demonstrated by Sherwood and colleagues [10, 11] in the rat. More recently, targeted gene deletion of relaxin ($Rln^{-/-}$) or the relaxin receptor ($Rxfp1^{-/-}$) provides direct evidence of the role of relaxin in tissue remodeling. The pubic symphysis of an $Rln^{-/-}$ pregnant female fails to elongate [12, 13]. In addition, both models display defects in the cervix, vagina, and mammary gland, resulting in prolonged or failed parturition and impaired nipple development [12, 14, 15].

The progressive modifications that occur in the mouse pubic joint during pregnancy are proposed to result from the cell-type switch of chondrocytes to fibroblasts and the resulting alterations in the composition and histoarchitecture of the ECM. Ultrastructural and immunohistochemical studies suggest that rearrangement of collagen and elastic fibers and changes in proteoglycan and hyaluronan (HA) composition at term are important in PS remodeling [16–21]. In addition, proteolytic enzymes such as matrix metalloprotease 2 and cathepsin K and B and tissue inhibitors of metalloproteases (TIMP1 and TIMP2) are proposed to contribute to symphysis relaxation [9, 16, 21–23]. There are multiple routes of regulation by which the tensile strength and flexibility of a tissue can be modified. These routes include 1) alterations in processing, assembly, and breakdown of collagen fibrils; 2) the presence or absence of specific matricellular proteins and proteoglycans, which regulate collagen fibril size, deposition in the matrix, and structure; and 3) the type, length, and degree of sulfation of the glycosaminoglycans (GAG) chain on proteoglycans.

While regulated changes in ECM components are proposed to contribute to PS remodeling, there are few quantitative data to support temporal changes in sulfated and nonsulfated glycosaminoglycans, proteoglycans, or matricellular proteins,

[1]R.G.R. was supported by a graduate studentship from Conselho Nacional de Desenvolvimento Científico e Tecnológico (CNPq; grant no. 141765/2007-0). This study was supported by grants from FAPESP (grant no. 05/51844-8 to R.G.R.), CNPq (grants 304910/2006-6 and 477535/2008-9 to R.G.R.), and U.S. National Institutes of Health grant P01 HD011149 (to M.M.).
[2]Correspondence: E-mail: mala.mahendroo@utsouthwestern.edu

Received: 31 May 2011.
First decision: 12 July 2011.
Accepted: 14 October 2011.

eISSN: 1529-7268 http://www.biolreprod.org
ISSN: 0006-3363

all of which can greatly influence the properties of the main structural protein fibrillar collagen. In addition, direct assessment of the types of fibrillar collagen and changes in collagen processing, structure, and content throughout pregnancy and postpartum have not been well defined and are critical to understand mechanisms of PS remodeling. To address these gaps in our understanding of PS remodeling, we measured temporal changes in collagen type, solubility, and abundance, quantified all GAGs in the PS, and defined key ECM components that contribute to IpL elongation at parturition.

MATERIALS AND METHODS

Mice

Animals were housed in a 12L:12D photoperiod (lights-on, 06:00–18:00 h) at 22°C. Mice were of mixed strains (C57B6/129Sv) or NIH Swiss mice. The C57B6/129Sv mice were generated and maintained as a breeder colony at the University of Texas Southwestern Medical Center (Dallas, TX), while the NIH Swiss mice were purchased from Harlan Laboratories (Indianapolis, IN). Mice in these studies were 3 to 6 mo old and nulliparous. Female mice were housed with males from 08:00 h to 16:00 h and then checked at 16:00 h for vaginal plugs. The day of plug formation was counted as d0, and birth occurred in the early morning of d19. Most samples were collected at mid-day unless otherwise specified. Samples indicated as late d18.75 were collected in the evening of d18, generally between 17:00 and 19:00 h. Postpartum samples were collected after birth at the indicated times. All studies were conducted in accordance with the standards of humane animal care as described in the U.S. National Institutes of Health (NIH) *Guide for the Care and Use of Laboratory Animals*. The research protocols were approved by the institutional animal care and research advisory committee. Pubic symphyses were collected from nonpregnant (NP) mice at time points during pregnancy (d10–d19 in labor), and after delivery at 2–4, 24, 48, and 72 h pp. Upon dissection, the medial portions of the PS bones or ligaments were removed for subsequent experimentation.

Collagen Content and Solubility

Pubic symphysis samples from NP and pregnant mice were weighed and lyophilized to enable measurement of their dry weight and water content. Dried samples were rehydrated for 1 h with 1 M NaCl buffer containing 1% proteinase inhibitor (Sigma, St. Louis, MO). Samples were homogenized using the Polytron homogenizer (Kinematica, Switzerland) and extracted at 4°C for 24 h with shaking. The samples were centrifuged at 4°C for 10 min at 16 000 × *g*, and the supernatant was removed from the pellet and frozen at −20°C. Pellets were subsequently extracted with 0.5 M acetic acid with 1% protease inhibitor at 4°C for 24 h and centrifuged, and the resulting pellet was further extracted with 0.5 M acetic acid containing pepsin (1 mg/ml) (Sigma) at 4°C for 24 h. The supernatants from each extraction and the final pellet were stored at −20°C. The amount of soluble collagen present in each fraction was measured by a colorimetric hydroxyproline assay. The supernatants and pellets were hydrolyzed in 6 M HCl at 110°C for 24 h, and the hydroxyproline assays were carried out as previously described [24]. The amount of total collagen was determined by using a mass ratio of collagen to hydroxyproline of 7.46:1 and was normalized to tissue dry weight. A minimal amount of collagen was detectable in the NaCl and acetic acid fractions, and thus, the soluble collagen was defined as a combination of collagen extracted in NaCl, in acetic acid alone, and in acetic acid containing pepsin.

Protein Blots

Collagen I and C-propeptide protein extraction. Frozen PS tissue was pulverized and then homogenized with a Polytron tissue homogenizer in 300 μl of cold 7 M urea buffer and 0.1 M sodium phosphate, pH 7.8, plus 1% protease inhibitor (Sigma) and extracted overnight at 4°C. Protein levels were quantified (BCA protein assay kit; Pierce, Rockford, IL).

Collagen dot blot. Protein used in dot blot analysis was extracted as described elsewhere [25] with some modifications. Briefly, PS tissues were homogenized in 300 μl of radio-immunoprecipitation assay buffer with protease inhibitors and agitated for 2 h at 4°C. Samples of 2.5 μg of protein were spotted onto a nitrocellulose membrane and probed with rabbit polyclonal anti-collagen I, rabbit polyclonal anti-collagen II, or rabbit polyclonal anti-collagen III primary antibody (codes ab34710, ab21291, and ab7778, respectively; Abcam, Cambridge, MA). Secondary antibody for both Western blotting and dot blotting was donkey anti-rabbit horseradish peroxidase (HRP; catalog no. 711036152; Jackson ImmunoResearch, Westgrove, PA). Chemiluminescence was visualized using ECL (GE Healthcare, Buckinghamshire, U.K.). Digital images of the blots were visualized and photographed using a Fuji film LAS-3000 chemiluminescence imager (Tokyo, Japan).

HA Western blotting. Western blotting was executed by using a biotinylated HA binding protein (HABP) as a probe as previously described with some modifications [26]. Specificity of HABP has previously been tested using samples treated with the HA-degrading enzyme, hyaluronidase. Single PS tissues were homogenized in 300 μl of cold 0.1 M PBS plus 1% protease inhibitor (Sigma). One third of the sample (100 μl) was ethanol precipitated and run on a 4%–15% gel. HA was detected by incubating the membrane with biotinylated HABP (0.5 μg/ml) for 2 h at room temperature (RT) (Seikagaku, Japan), followed by HRP-conjugated streptavidin. Positive bands were visualized using ECL detection reagent, and proteins were visualized using a Fuji film LAS-3000 chemiluminescence imager.

Decorin protein extraction. Pulverized PS tissue was homogenized and extracted for 48 h in 1 ml of 4 M guanidine hydrochloride containing 1% proteinase inhibitor at 4°C. Samples were dialyzed in 0.1 M NaCL and 0.1 M Tris-HCl, pH 7.3. After dialysis, protein concentration was determined by using BCA protein assay. Twenty micrograms of protein were treated with and without chondroitinase ABC (10 mU/μl; Seikagaku) and incubated at 37°C for 2 h. Samples were precipitated in 100% ethanol at −20°C for 2 h and centrifuged at 4°C. The resulting pellet was resuspended in Laemmli buffer.

A total of 10–20 μg of protein was used for collagen I alpha1, collagen C-propeptide, or decorin blots. Each sample was boiled for 5 min in reducing Laemmli buffer and analyzed by SDS-PAGE on 4%–20% Tris HCl precast gels (Bio-Rad, Hercules, CA), along with protein standards (Precision Plus protein Kaleidoscope; Bio-Rad). Proteins were transferred onto nitrocellulose membrane (Biotrace Pall Life Sciences, Pensacola, FL). Membranes were blocked for 2 h at RT in 3% skim milk, 0.05% Tween in Tris-buffered saline (TBS). Blots were then incubated for 2 h with primary antibody (rabbit anti-collagen Ia1, 1:1000 dilution [MD Biosciences]; rabbit anti-collagen C-propeptide, 1:1000 dilution [LF-41]; or rabbit anti-decorin, 1:3000 dilution [LF-113]; LF-41 and LF-113 were gifts from Larry Fisher, NIH) in blocking solution, washed in TBS with Tween (TBST), incubated with HRP-labeled anti-rabbit immunoglobulin G (IgG; 1:10 000 dilution; Jackson ImmunoResearch Labs, Westgrove, PA) for 45 min at RT and washed again in TBST. Positive bands were visualized using ECL Western blotting detection reagents (Amersham Biosciences).

Protein blots for THBS2 and SPARC. Pulverized tissue was homogenized in radio-immunoprecipitation assay buffer (150 mM NaCl, 10 mM Tris, pH7.2, 0.1% SDS, 1.0% Triton X-100, 1% DOCA, and 5 mM EDTA) plus 1.5% protease inhibitor cocktail (Sigma-Aldrich). Protein concentration of supernatants was determined as described above. Twenty micrograms of protein were analyzed by SDS-PAGE on a 4%–20% gel and transferred to a polyvinylidene fluoride membrane at 100 V for 1 h at 4°C. The membrane was blocked using 5% milk in TBST for 1 h and then probed with a purified mouse anti-mouse thrombospondin 2 (THBS2; 1:1000 dilution; BD Biosciences) or a mouse anti-secreted protein acidic and rich in cysteine (SPARC) monoclonal antibody (1:500 dilution; reagent provided by Rolf Brekken, UT Southwestern Medical Center, Dallas, TX) overnight at 4°C. The secondary antibody-HRP-conjugated goat anti-mouse IgG (1:5000 dilution; Bio-Rad) was incubated for 1 h at RT. A 200-kDa band (THBS2) and a 45-kDa band (SPARC) were visualized using ECL Western blotting detection agents (GE Healthcare). The blot was probed with glyceraldehyde-3-phosphate dehydrogenase (GAPDH; 1:1000 dilution; Santa Cruz Biotechnology, Inc., CA) to assess protein loading.

Fluorophore-Assisted Carbohydrate Electrophoresis

One PS per time point was lyophilized overnight, and wet and dry weights were determined before and after lyophilization, respectively. Tissues were then digested in 100 mM ammonium acetate with 0.0005% phenol red (pH 7) containing 0.25 mg/ml proteinase K (Roche, Indianapolis, IN) for 4 h at 60°C. Proteinase K was inactivated by boiling at 100°C for 10 min. A 12.5-μl aliquot of the supernatant equal to 0.125 mg dry weight of digested PS was processed for fluorophore-assisted carbohydrate electrophoresis (FACE) analysis as described elsewhere with minor modifications [27, 28].

HA and chondroitin sulfate and dermatin sulfate (CS/DS) disaccharides were generated by digestion with hyaluronidase streptococcus dysgalactiae (10 mU) at 37°C for 1 h, followed by chondroitinase ABC (10 mU) for 2 h. Heparan sulfate (HS) was broken down into disaccharides by digestion with a mixture of heparitinase and heparitinase 1 and 2 (2.5 mU per enzyme) at 37°C for 3 h. Keratin sulfate (KS) disaccharides were generated by keratinase II (5 mU) incubation for 3 h at 37°C. Enzymes were obtained from Associates of Cape Cod, East Falmouth, MA. Enzymes were then inactivated by boiling for 5 min. Digests of HA, CS/DS, or KS disaccharides were fluorescently labeled by addition of 5 μl of 25 mM 2-aminoacridone (Invitrogen, Carlsbad, CA) dissolved in 85% dimethyl sulfoxide and 15% acetic acid and incubation for 15

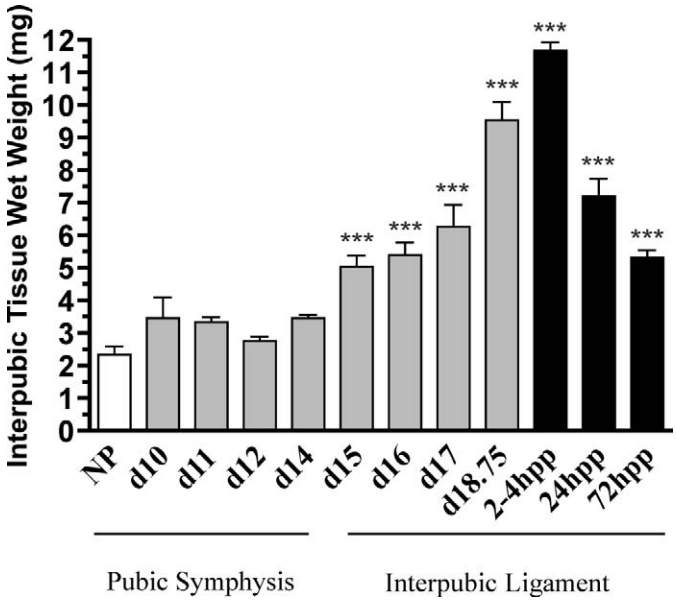

FIG. 1. Wet weight of interpubic tissue is increased toward the end of pregnancy. PS (NP and d10–d12) and IpL (d14–d18.75 and pp 2–4, 24, and 72 [hpp]). Each column represents the mean ± SEM. N = 3–20/group. ***Significant difference compared to NP ($P < 0.01$).

min at RT. Samples were incubated overnight at 37°C with 5 μl of 2.5 M NaCNBH4. Following overnight incubation at 37°C, 2.5 μl of glycerol was added, and the sample was stored at −80°C. Sample and quantitative disaccharide standards were run on Glyko FACE monosaccharide composition gels (Prozyme, Hayward, CA) at a constant voltage of 500 V. Gels were imaged using a Fuji FLA-5000 Phosphorimager. Individual GAGs were quantified from scanned gels by using Fujifilm Multigauge 3.0 software.

HA Molecular Weight Gels

HA molecular weight was determined as described previously with minor modifications [26]. Specificity of Stains All (Sigma) for HA has previously been tested using samples treated with the HA-degrading enzyme, hyaluronidase. An aliquot equal to 0.4 mg dry weight of proteinase K digested tissue (as described in the section above) was treated with 3 μl of DNase (Ambion, Austin, Texas) and 3 μl of RNase A (1.28 mg/ml; Roche) for 5 h at 37°C. Samples were boiled for 5 min to inactivate enzymes. GAGs were precipitated in ethanol at −20°C overnight and pelleted by centrifugation at 16 000 × *g* for 10 min. Pellets were resuspended in 15 μl of TAE buffer (Tris-sodium acetate-EDTA, pH 7.9) and 3 μl of loading buffer (0.2% bromophenol blue, 1 ml TAE buffer, and 8.5 ml glycerol). Samples were run on a 1% agarose gel (Seakem HGT; Cambrex, Rockland, ME) made in TAE buffer. The gel was pre-run for ~4 h at 80 V, and running buffer was replaced with fresh TAE before samples and HA size standards (Hyalose, Oklahoma City, OK) were loaded. Gel was run at 100 V. After electrophoresis, the gel was equilibrated in 30% ethanol for ~30 min with shaking at RT, followed by incubation in 2.5 mg/ml Stains All solution (Sigma) overnight in the dark. Gel was destained in water until bands were visualized before scanning.

RNA Isolation and Quantitative Real-Time PCR

Total RNA was extracted from frozen mouse tissue using RNA Stat 60 (Tel-Test Inc., Friendswood, TX) and treated with DNase I to remove any genomic DNA (DNA-Free; Ambion). Complementary DNA synthesis was performed using 2 μg of total RNA in a 100-μl volume (TaqMan cDNA synthesis kit; Applied Biosystems, Foster City, CA). Quantitative real-time PCR (qRTPCR) was performed using SYBR Green and a PRISM7900HT sequence detection system (Applied Biosystems). Aliquots (20 ng) of cDNA were used for each qPCR, and each reaction was run in triplicate. Each gene was normalized to the expression of the housekeeping gene 36B4 (official symbol, *Rplp0*) [29], and expression was calculated relative to that of d = (d18.75) pubic symphyses as the external calibrator in the $2^{-\Delta\Delta Ct}$ method, as described in Applied Biosystems *User Bulletin No. 2*. Data are presented as the average relative gene expression ± SEM. Supplemental Table S1 (available online at www.biolreprod.org) indicates primer sequences for each gene assessed. Primers for versican recognize the V0 and V1 isoforms.

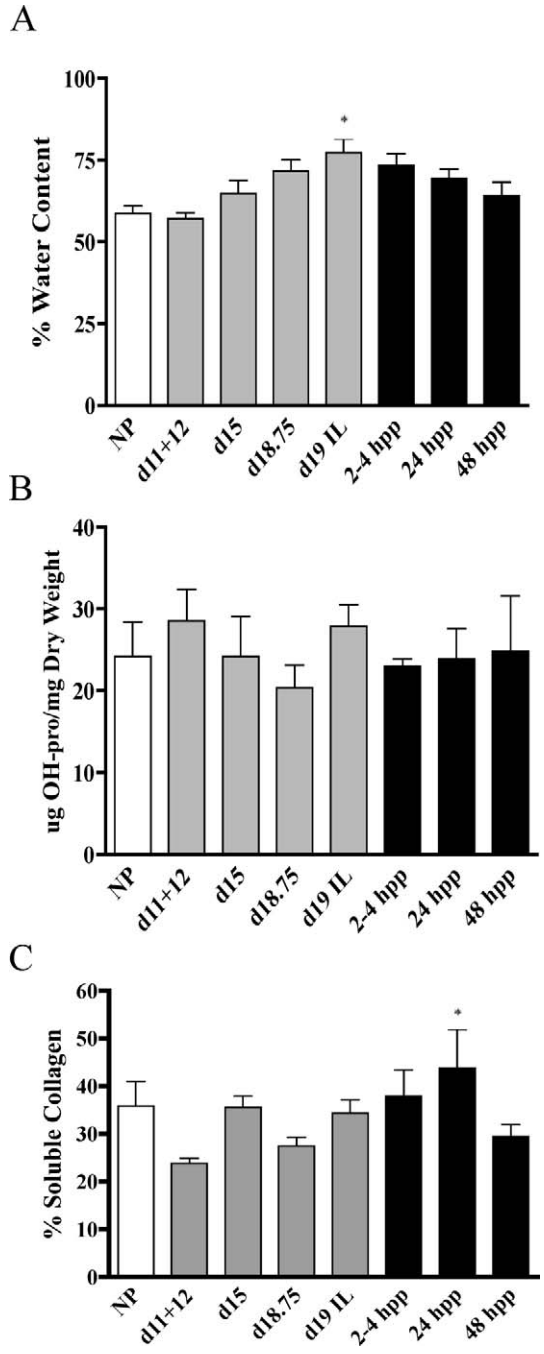

FIG. 2. Water, total collagen, and soluble collagen contents were measured using PS (NP and d11–d12) and IpL (d15, d18.75, and d19–in labor [IL] and pp 2–4, 24, and 48 h [hpp]). **A**) Water content is defined as the difference between the wet and dry tissue weight (mg) and is expressed as a percentage. **B**) Collagen content was normalized to dry tissue weight. **C**) The percentage of soluble collagen. Significance compared to d11+d12 (a pooled sample containing both d11 and d12 tissue) is indicated by a * ($P < 0.05$). N = 4–7/group. Data represent means ± SEM.

Statistical Analysis

Data were analyzed using one-way ANOVA with pair-wise multiple comparisons performed with Tukey test for data normally distributed. Data are displayed as the means ± SEM. P values <0.05 were considered statistically significant.

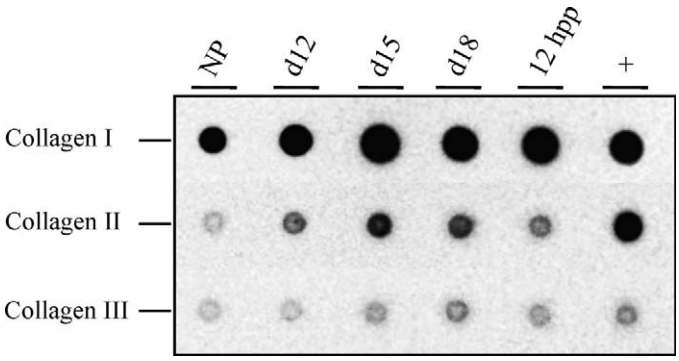

FIG. 3. Protein dot blotting to assess relative changes in collagen I, II, and III in the NP, d12, d15, and d18, and 12 h pp (hpp) PS. Femoral cartilage serves as a positive control (+). This experiment was carried out using two independent sets of tissue, and a representative blot is indicated. Images for all three blots were taken at the same exposure time to allow qualitative assessment of abundance.

RESULTS

PS and IpL Tissue Wet Weight

PS/IpL was collected from NP and pregnant mice at d10, d11, d12, d14, d15, d16, d17, and late day 18.75 and at 2–4, 24, and 72 h pp. The transition from PS to IpL on d14 is characterized by a gradual increase in wet weight, which is maximal at 2–4 h pp and then declines thereafter as the tissue remodels from a ligament to PS (Fig. 1).

Water Content, Collagen Content, and Solubility

The increased growth and flexibility of the pubic ligament at term may result from increased hydration and changes in the abundance or structure of total collagen. Water content was measured in NP, pregnant, and pp interpubic samples.

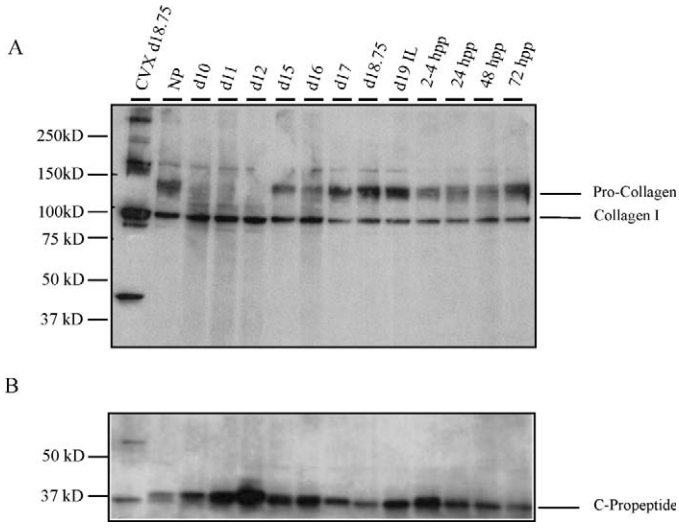

FIG. 4. **A**) The abundance of extractable collagen was evaluated by Western blotting using an antibody specific for collagen type I alpha1 in urea-extracted protein from PS (NP and d10–d12), IpL (d15–d18.75, d19 IL, and pp 2–4, 24, 48, and 72 h [hpp]). Procollagen migrates at 125 kDa, while mature collagen migrates at 100 kDa. Cervix was used as a positive control. **B**) Collagen processing at the C terminus was evaluated in Western blotting using a C-propeptide-specific antibody (a gift from Dr. Larry Fisher, NIH). PS was evaluated at time points described in **A**. Experiments were performed three times, and a representative blot is presented.

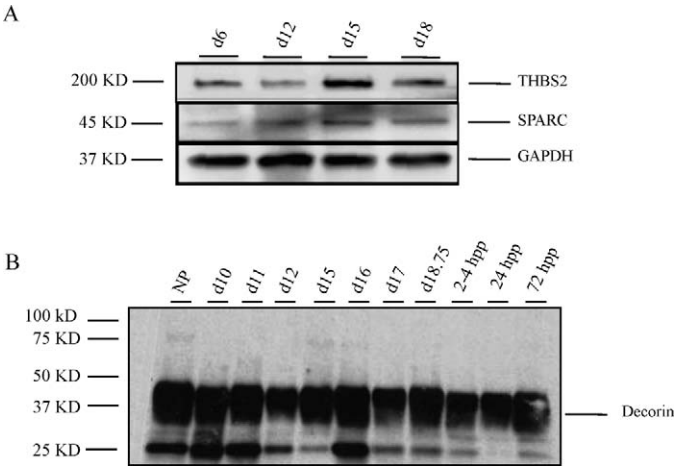

FIG. 5. Matricellular proteins and decorin are expressed in the PS and IpL throughout pregnancy. **A**) THBS2 and SPARC are expressed in the PS (NP, d6, d12) and IpL (d15 and 18.75). GAPDH is a loading control. Experiment was performed four times and a representative blot is presented. **B**) Decorin expression in the PS (NP, d10–d12) and IpL (d15–d18.75 and pp 2–4, 24, and 72 h [hpp]).

Compared to NP (59%) samples, there was a gradual increase in water content, which reached statistical significance by d19 in labor (IL) (78%) and declined thereafter (Fig. 2A). By 48 h pp, the water content was similar to that of NP. Total collagen content was evaluated by hydroxyproline measurement and normalized to tissue dry weight. The abundance levels of total collagen were similar in interpubic tissues from NP, pregnant, and pp samples (Fig. 2B). The solubility of collagen in acid solutions can be used as an indirect measure to evaluate alterations in collagen processing and assembly, as mature processed collagen has low solubility. Compared to nonpregnant PS, there was no significant change in collagen solubility throughout pregnancy. Solubility modestly increased at 24 h pp and returned to normal levels by 48 h pp (Fig. 2C).

Assessment of Fibrillar Collagens

Fibril collagen type I is the primary collagen present in the symphysis as reported in the rat [30]. In the current study, we sought to determine the relative changes in fibril collagens I, II, and III in the mouse PS. Protein dot blotting was performed using antibodies specific for all three collagens. Compared to the NP sample, there appeared to be modest increases in collagens I and II during pregnancy, while collagen III expression remained constant in NP, pregnant, and pp PS (Fig. 3). Given possible differences in antibody affinities, the relative expression of each collagen cannot be quantified; however, one can qualitatively estimate collagen I to be the most abundant fibrillar collagen, followed by collagen II and then III.

Collagen I

Further assessment of collagen I was carried out in the PS during pregnancy. During processing, N- and C-terminal propeptides are cleaved from procollagen to form mature collagen. The abundance of urea-extractable collagen I was assessed in NP, pregnant tissue, and pp PS and IpL. Protein blotting using a collagen I antibody that recognizes mature collagen (100 kDa) as well as procollagen revealed similar levels of extractable mature collagen at all time points, while procollagen migrating at 125 kDa was most abundant in the

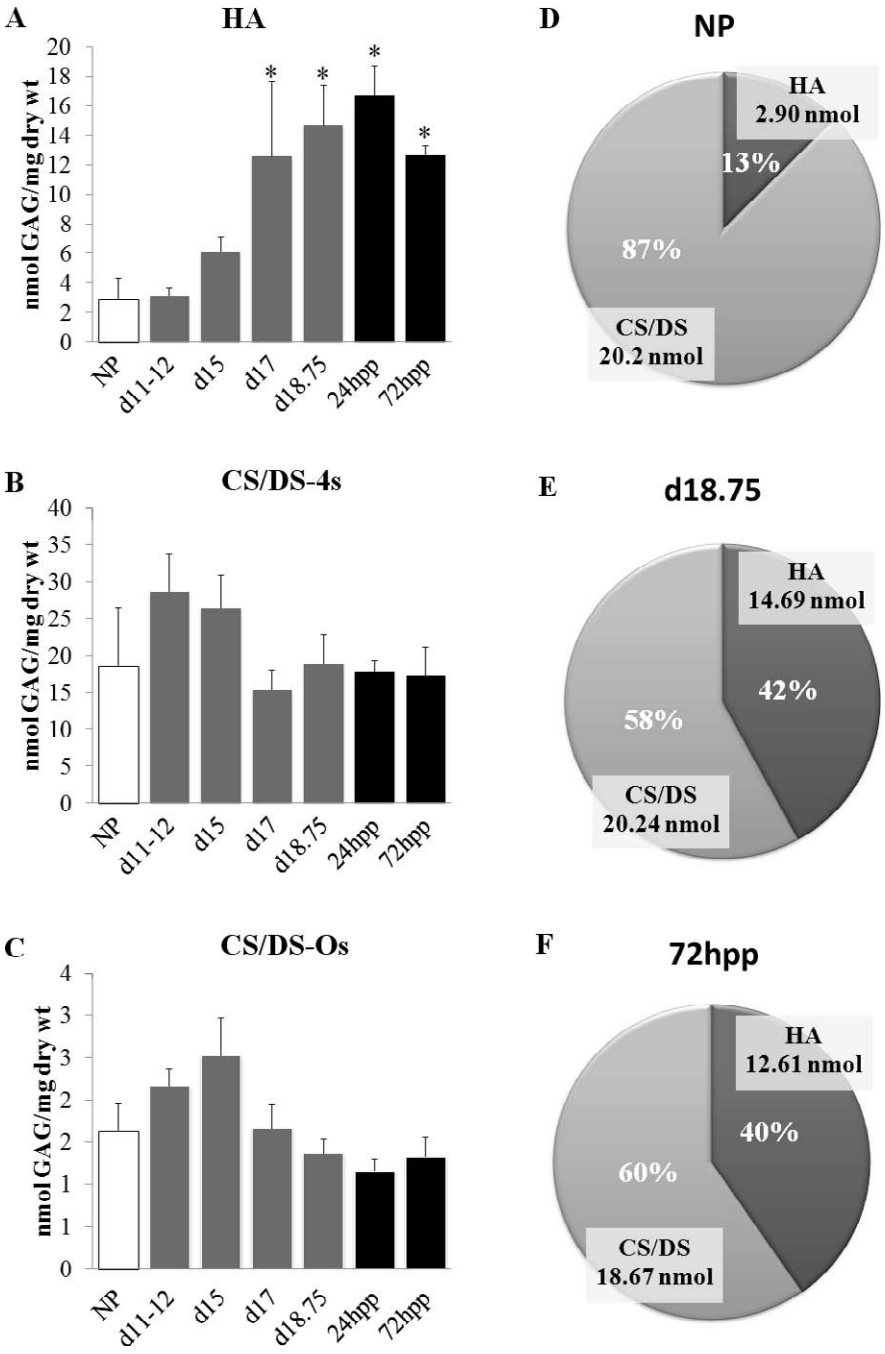

FIG. 6. HA but not CS/DS GAGs is elevated in the IpL at term. PS was collected from NP, d11–d18, and pp 72 h (hpp) mice. **A**) Quantitative assessment of HA, n = 4–5/group. **B**) Quantitative assessment of CS/DS 4s, n = 4–5/group. **C**) Quantitative assessment of CS/DS- 0s, n = 4–5/group. **D–F)** Pie charts indicate relative percentage of GAGs in NP, d18.75, and 72 h pp. Data represent means ± SEM; $*P < 0.05$ compared to NP.

IpL from d15 onward. While mature collagen appears somewhat reduced in abundance from d15 onward, this was not significant. Cervix was used as a positive control, and an unidentified band migrating at 50 kDa was observed that lacked the PS (Fig. 4A). To determine if the increased presence of procollagen in pregnant and pp IpL resulted from a decline in processing of the C-terminal propeptide, we performed Western blotting using a C-propeptide-specific antibody. Blots revealed the presence of the C-propeptide at all time points (Fig. 4B). No significant changes in expression were observed, suggesting normal processing of the C terminus. A commercial antibody against the N-terminal propeptide was not effective in our hands, thus, we were unable to assess N-terminal processing at this time (Pro-col1a; code, sc-30136; Santa Cruz Biotechnology).

Matricellular Proteins, Proteoglycans, and GAGs

Components of the ECM such as matricellular proteins, proteoglycans, and GAGs can also play a role in collagen structure and organization. The expression of two matricellular proteins, THBS2 and SPARC, with functions in collagen fibrillogenesis and matrix deposition, respectively, were evaluated in the PS/IpL. As seen in Figure 5A, both proteins are expressed in the NP and pregnant PS/IpL, with no change

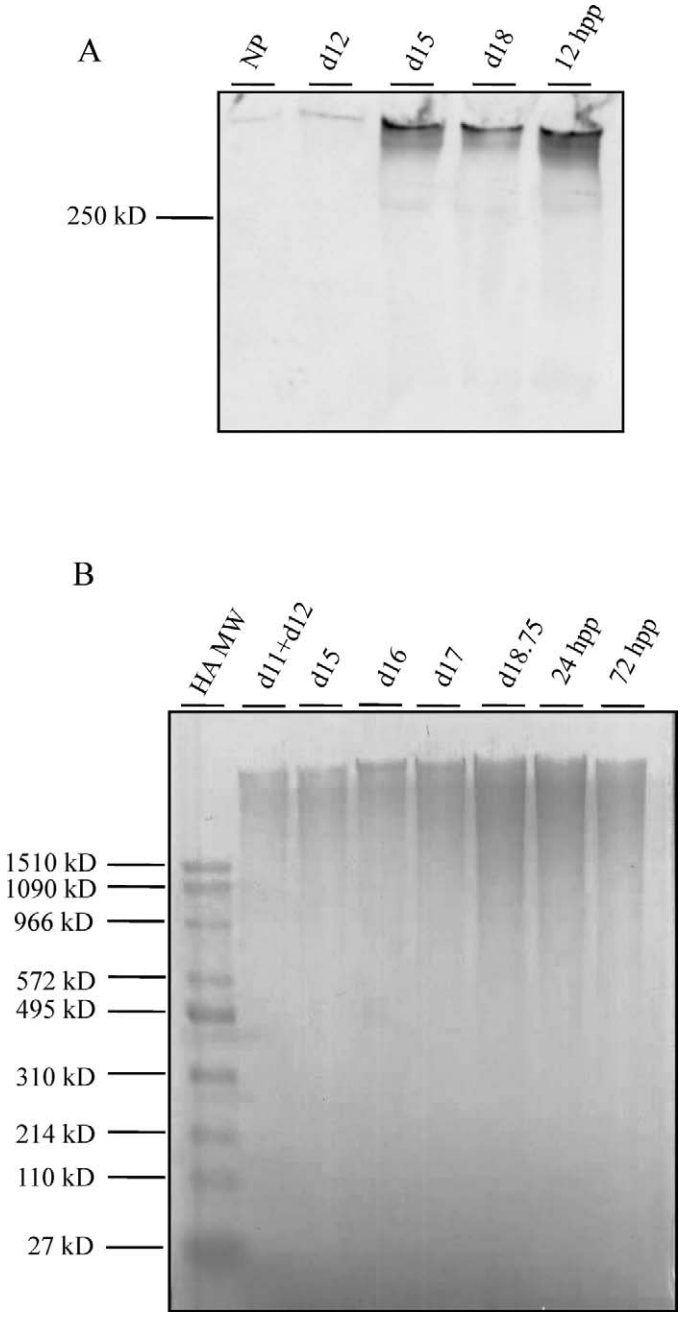

FIG. 7. **A**) Assessment of HA abundance by Western blotting using a biotinylated HABP as a probe (NP; d12, d15, and d18; and 12 h pp). **B**) Assessment of HA molecular weight during pregnancy and pp. Equal fractions of digested interpubic tissues from d11+d12, d15, d16, d17, and d18.75 and 24 h, and 72 h pp were analyzed using Stains All to visualize HA. HA molecular weight standards are indicated to the left of the gel.

in abundance. The proteoglycan decorin, which has functions in collagen fibrillogenesis, is also expressed in the PS\IpL at similar levels in the NP, pregnant, and pp tissue (Fig. 5B).

To identify and quantify GAGs in the PS/IpL, FACE was performed to quantify changes in all GAGs that include HA, CS/DS, HS, and KS. HA content is significantly increased by d17 compared to that of NP (Fig. 6A). Conversely, both CS/DS 4-sulfate (Fig. 6B) and CS/DS 0-sulfate (Fig. 6C) GAG expression levels in the PS and IpL were constant throughout gestation. The expression of HS and KS was also measured on d15 and d18 IpL. While low expression of HS was detected, KS was undetectable (data not shown). Thus, in the PS, CS/DS are the primary sulfated GAGs. Because many GAG chains are hybrids that contain both DS and CS on the same chain, it is not possible to distinguish differences in the levels of these two GAGs. The marked increase in HA at the end of pregnancy while CS and DS levels remain relatively constant results in a dynamic shift in the relative proportion of these GAGs (Fig. 6, D, E, and F).

The marked increase in HA levels in late gestation was further confirmed by Western blotting using a biotinylated HABP as a probe, as previously described [26]. As seen in Figure 7A, there was a gradual increase in HA content from NP to d18, with a maximum at d18 and pp.

HA functions are dependent in part on its size. To elucidate the potential functions of HA in PS remodeling, temporal changes in HA molecular weight in the PS and IpL were evaluated (Fig. 7B). Samples were run on agarose gels along with HA high (1510–495 kDa) and low (495–27 kDa) molecular weight standards. HA was detectable at all time points, with peak expression 1 day prior to birth (d18.75) and shortly pp. At all time points, the HA appeared to be a predominantly high molecular weight HA (>1510 kDa).

Gene Expression Studies

The increased production of high molecular weight HA in the IpL at the end of pregnancy must arise from regulated changes in expression of one or more of the HA synthase genes (*Has1*, *Has2*, *Has3*) or the hyaluronidase genes (*Hyal1*, *Hyal2*) that break down HA. qRTPCR was performed to evaluate gene expression in the mouse PS during pregnancy (d11+d12, d15, and d18.75) and pp (2–4 h pp and 24 h pp). *Has1* was expressed at all time points, with maximal induction at d18.75 (Fig. 8A). *Has2* expression was also increased on d18.75 but, in contrast to *Has1*, remained elevated at 2–4 h pp and decreased by 24 h pp (Fig. 8B). *Has3* had low to undetectable expression in PS tissue (data not shown). Both *Hyal1* and *Hyal2* were expressed in the PS and IpL. *Hyal1* had unaltered expression throughout gestation (Fig. 8C), while *Hyal2* was transiently increased on d18.75 compared to the period of PS tissue changes at d11+d12 and d15 (Fig. 8D).

In other tissues, HA is stabilized in the ECM by forming cross-links with the large proteoglycan, versican. While four isoforms of versican exist (V0, V1, V2, and V3), only isoforms V0 and V1 can interact with HA. These cross-links can be disrupted by members of a disintegrin-like and metalloprotease with thrombospondin type 1 (ADAMTS) motif protease family such as ADAMTS1 and ADAMTS4 [30]. qRTPCR using primers that recognize the isoforms V0 and V1 reveals that versican (Fig. 9A) is expressed at low levels in the early pregnant PS and that expression is increased in the IpL with maximal expression prior to birth. Levels decline rapidly pp. ADAMTS1 had a relatively high expression in NP and early pregnancy tissues with a marked decline in expression by d15 and d18, as seen by Western blotting (Fig. 9B).

DISCUSSION

Current studies reveal the fact that expansion of the IpL in the mouse results from increased synthesis and secretion of a unique ECM by newly formed fibroblasts. This matrix is abundant in HA and the CS/DS-containing proteoglycans versican and decorin. While an increase in HA has previously been reported in the term pregnant IpL [17], the current study enhances our understanding by providing quantitative assessment of all GAGs in the PS including HA; determines the

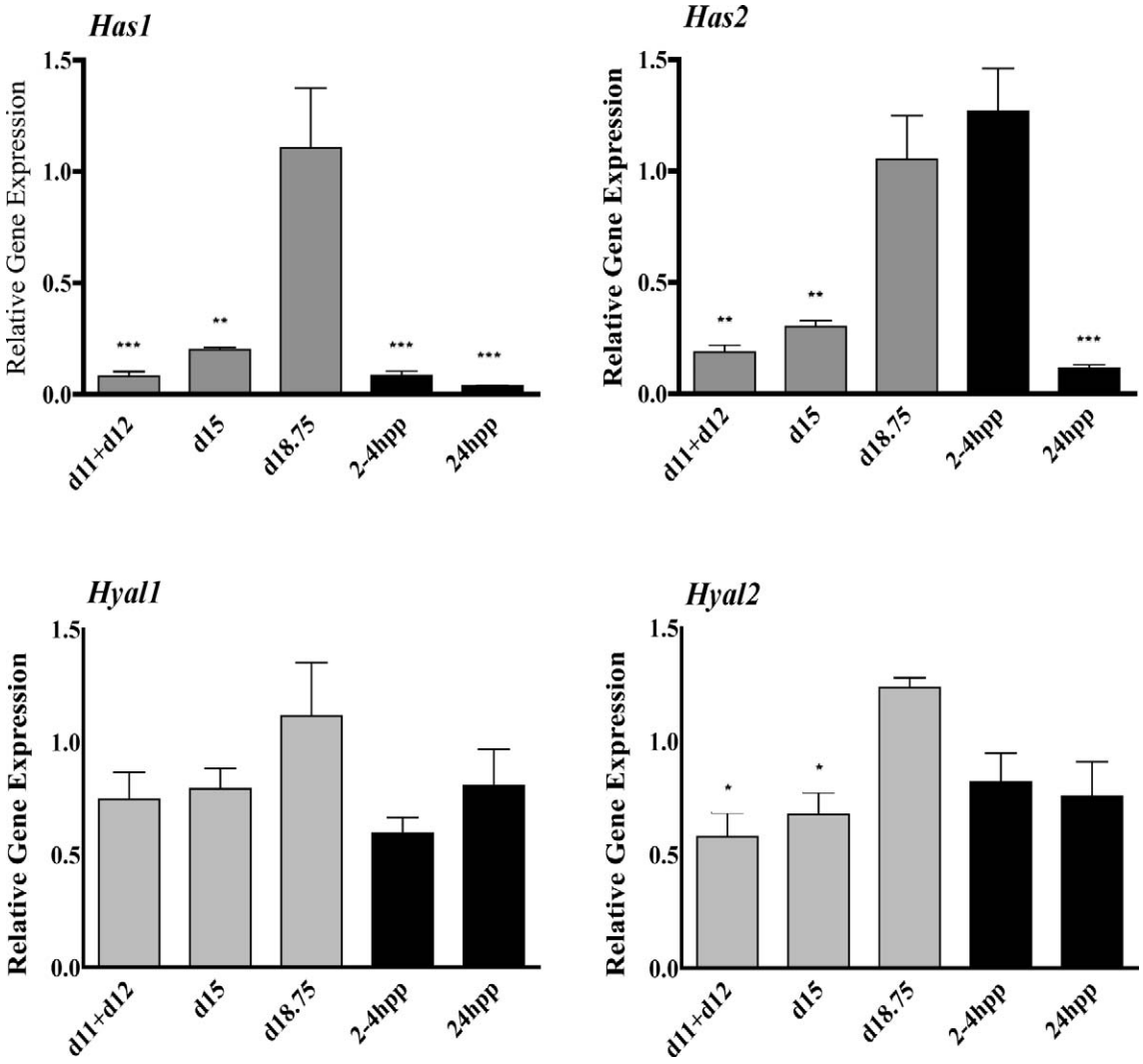

FIG. 8. Assessment of gene expression for *Has1* (**A**), *Has2* (**B**), *Hyal1* (**C**), and *Hyal2* (**D**) in pregnant and pp interpubic tissue by qRTPCR. Relative expression was quantified and normalized to the housekeeping gene 36B4 (official symbol *Rplp0*). Data represent means ± SEM of four IpL (d15 and d18.75 and 2–4 h pp and 24 h pp) and eight PS samples (each sample was a pool of 1–d11 and 1–d12). $^{*}P < 0.05$, $^{**}P < 0.01$, and $^{***}P < 0.001$ compared with d18.75 for all genes analyzed.

relative proportion of HA to CS/DS through pregnancy; elucidates HA size, which impacts its function; and identifies the HA synthase isozymes regulated in the IpL. Furthermore, we provide evidence that maximal expansion and flexibility of the IpL at the time of labor is not achieved by loss of total collagen, change in the relative ratio of fibril collagens I, II, and III, or changes in C-terminal processing of collagen I. Based on the continued synthesis and processing of procollagen I in the IpL, as shown in this study, and simultaneous degradation of the fibers by matrix metalloproteases, as previously described [22], we suggest a high turnover of collagen during pregnancy in the IpL, resulting in a high proportion of newly synthesized collagen in the ECM. These findings lead us to propose a model in which increased synthesis of high molecular weight HA and versican, along with a decline in the versican-degrading enzyme ADAMTS1, serves to promote tissue hydration, collagen disarray, and increased tissue viscoelasticity.

Quantitative assessment of GAGs reveals a marked increase in HA from 13% of total GAGs in NP to 42% of GAGs late on d18. Chondroitin and dermatan sulfated GAGs are the only sulfated GAGs in the PS and IpL, as heparan and keratin sulfated GAGs were undetectable. This observation is consistent with those of previous studies of the NP PS [20, 31].

CS/DS chains exist as single-sulfated 0-S and 4-S GAGs, and neither form changes significantly over the course of pregnancy. This finding is important to note as the degree of sulfation can alter proteoglycan function with respect to growth factor binding and cell signaling properties [32]. While CS/DS levels remain constant, they account for a significantly reduced proportion of total GAGs in pregnancy.

Consistent with the presence of CS/DS GAGs, two CS/DS-containing proteoglycans, decorin and versican, are expressed in the PS/IpL. Decorin expression was unchanged, suggesting that the loss of decorin is not a key physiological process required for modulation of collagen fibrillogenesis during IpL remodeling and elongation. While CS/DS GAGs remain constant, transcripts encoding versican are increased, suggesting there could be a reduction in GAG chain length or GAG attachment to the versican protein core. Further studies are required in which GAG chains will be analyzed after purification of individual proteoglycans. In addition, both the THBS2 and SPARC matricellular proteins had constant expression in the PS and IpL, suggesting that these proteins

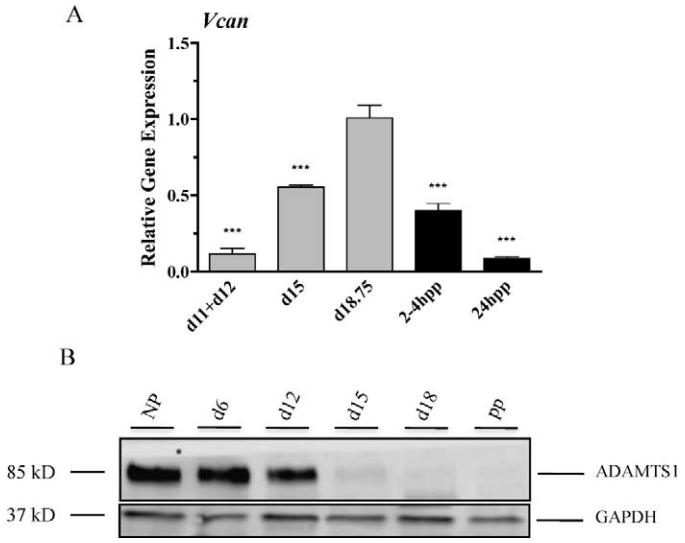

FIG. 9. **A**) Versican (*Vcan*) transcripts were evaluated by qRTPCR as described in Figure 8. Data represent means ± SEM of four IpL (d15 and d18.75 and 2–4 h pp and 24 h pp) and eight PS samples (each sample was a pool of 1–d11 and 1–d12); $***P < 0.001$ compared to d18.75. **B**) ADAMTS1 expression declines in the IpL at term. NP, d6, d12, d15, and d18 of gestation, and pp is ≈24 h pp. GAPDH was used as a loading control. Experiments were performed four times, and a representative blot is presented.

do not facilitate changes in collagen fibrillogenesis or matrix deposition during IpL formation or elongation [33, 34].

Important insights into the potential functions of HA and versican arise from the observations that HA in the IpL is primarily of large molecular weight (>1510 kDa) and that versican mRNA expression increases while ADAMTS1 protein expression is abolished by d18. The functions of HA are dependent in part on the size of the HA [35, 36]. Large molecular weight HA is space filling and promotes tissue hydration and matrix disorganization, in contrast to low molecular weight HA, which has proinflammatory functions [36]. Versican stabilization of HA matrices is crucial in other biological processes, such as in heart development. Genetic loss of either versican or HA synthase 2 results in embryonic lethality due to inappropriate heart formation [37, 38]. The breakdown of HA-versican matrices can be facilitated by the HA-degrading enzyme hyaluronidase or members of the ADAMTS family [39, 40–42]. While there was a small but significant increase in transcripts encoding *Hyal2*, the majority of HA appeared as high molecular weight products. This suggests that *Hyal2* activity remains low. The concomitant increase in versican transcripts and downregulation of ADAMTS1 expression in late pregnancy is likely to result in increased availability of versican to interact with HA. This interaction promotes stabilization of the HA-rich matrix that functions as a space-filling molecule to promote collagen disorganization/reorganization and to increase tissue hydration and viscoelasticity, resulting in IpL elongation.

Similar to the IpL, the cervix is a connective-rich tissue in which tissue remodeling and cell proliferation during pregnancy are regulated by relaxin and steroid hormones [5, 43, 44]. Similar to IpL elongation, cervical ripening is not mediated by an influx of neutrophils that secrete ECM-degrading enzymes nor by a decline in collagen content but is characterized by increased HA synthesis [9, 25, 26, 45–49]. While many processes appear conserved, the current study reveals novel differences that suggest distinct mechanisms in IpL elongation versus cervical ripening in preparation for labor and birth. The decline in cervical expression of *Thbs2* and increase in SPARC matricellular proteins were not evident in the PS, where expression was low and constant during pregnancy [25]. Most notable was the increased synthesis of high molecular weight HA and versican along with a decline in expression of the protease ADAMTS1 in the IpL on d18. These patterns of expression are consistent with a stabilized HA-rich matrix that will facilitate flexibility of the pubic symphysis to allow sufficient opening of the birth canal during parturition. In the term cervix, there is a greater size distribution of HA, which ranges from high to medium molecular weight [26]. Versican is also expressed, yet expression of the protease ADAMTS1 and hyaluronidase activity increases at term (Akgul and Mahendroo, unpublished results) [26]. This differing pattern of expression in the cervix may serve to initially promote a stabilized HA matrix for increased tissue viscoelasticity in early ripening, which is followed by a loss of HA-versican matrices and loss of tissue integrity, to allow maximal cervical opening with onset of uterine contractions during birth [48]. These tissue-specific differences may arise from differential regulation of these factors by fibroblasts in the IpL versus fibroblasts or other cells in the cervix and fine tune the biomechanical properties required for IpL flexibility versus cervical ripening and dilation.

PS remodeling is an important component of the parturition process, and the current study enhances our understanding of the dynamic changes in the ECM that mediate this process. Future studies will determine if the changes in HA and versican are sufficient or necessary for IpL elongation, and they will focus on the regulation of the IpL ECM composition by the interaction of relaxin with its receptor RXFP1.

ACKNOWLEDGMENT

We thank Meredith Akins for critical reading of the manuscript. We also thank Jianfeng Ye, Meredith Akins, Ph.D., Brenda Timmons, Ph.D., and Anjana Tiwari, Ph.D., for help with the procedures and analyses. We thank Dr. Larry Fisher, NIH, who kindly provided decorin and C-propeptide antibodies used in this work, and Dr. Rolf Brekken, who provided SPARC antibody. This work was part of a dissertation submitted by R.G.R. to the Institute of Biology, State University of Campinas (UNICAMP), in partial fulfillment of the requirements for a Ph.D. degree.

REFERENCES

1. Crelin ES. The effect of estrogen and relaxin on intact and transplanted pubic symphyses in mice. Anat Rec 1954; 118:380–381.
2. Hall K. The effects of pregnancy and relaxin on the histology of the pubic symphysis in the mouse. J Endocrinol 1947; 5:174–182.
3. Ruth EB. Metamorphosis of the pubic symphysis. III: Histological changes in the symphysis of the pregnant guinea pig. Anat Rec 1937; 67:409–421.
4. Becker I, Woodley SJ, Stringer MD. The adult human pubic symphysis: a systematic review. J Anat 2010; 217:475–487.
5. Bjorklund K, Bergström S, Nordström ML, Ulmsten U. Symphyseal distention in relation to serum relaxin levels and pelvic pain in pregnancy. Acta Obstet Gynecol Scand 2000; 79:269–275.
6. Davidson MR. Examining separated symphysis pubis. J Nurse Midwifery 1996; 41:259–262.
7. Veridiano AM, Garcia EA, Pinheiro MC, Nishimori FY, Toledo OMS, Joazeiro PP. The mouse pubic symphysis as a remodeling system: morphometrical analysis of proliferation and cell death during pregnancy, partus and postpartum. Cell Tissue Res 2007; 330:161–167.
8. Moraes SG, Pinheiro MC, Toledo OMS, Joazeiro P. Phenotypic modulation of fibroblastic cells in mice pubic symphysis during pregnancy, partum and postpartum. Cell Tissue Res 2004; 315:223–231.
9. Rosa RG, Tarsitano CA, Hyslop S, Yamada AT, Toledo OM, Joazeiro PP. Relaxation of the mouse pubic symphysis during late pregnancy is not

accompanied by the influx of granulocytes. Microsc Res Tech 2008; 71:169–178.
10. Downing SJ, Sherwood OD. The physiological role of relaxin in the pregnant rat. III. The influence of relaxin on cervical extensibility. Endocrinology 1985; 116:1215–1220.
11. Hwang JJ, Sherwood OD. Monoclonal antibodies specific for rat relaxin. III. Passive immunization with monoclonal antibodies throughout the second half of pregnancy reduces cervical growth and extensibility in intact rats. Endocrinology 1988; 123:2486–2490.
12. Zhao L, Roche PJ, Gunnersen JM, Hammond VE, Tregear GW, Wintour EM, Beck F. Mice without a functional relaxin gene are unable to deliver milk to their pups. Endocrinology 1999; 140:445–453.
13. Zhao L, Samuel CS, Tregear GW, Beck F, Wintour EM. Collagen studies in late pregnant relaxin null mice. Biol Reprod 2000; 63:697–703.
14. Kamat AA, Feng S, Bogatcheva NV, Truong A, Bishop CE, Agoulnik AI. Genetic targeting of relaxin and insulin-like factor 3 receptors in mice. Endocrinology 2004; 145:4712–4720.
15. Krajnc-Franken MA, van Disseldorp AJ, Koenders JE, Mosselman S, van Duin M, Gossen JA. Impaired nipple development and parturition in LGR7 knockout mice. Mol Cell Biol 2004; 24:687–696.
16. Wahl LM, Blandau RJ, Page RC. Effect of hormones on collagen metabolism and collagenase activity in the pubic symphysis ligament of the guinea pig. Endocrinology 1977; 100:571–579.
17. Garcia EA, Veridiano AM, Martins JR, Nader HB, Pinheiro MC, Joazeiro PP, Toledo OM. Hyaluronan involvement in the changes of mouse interpubic tissue during late pregnancy and post-partum. Cell Biol Int 2008; 32:913–919.
18. Moraes SG, Pinheiro MC, Yamada AT, Toledo OMS, Joazeiro PP. Differential distribution of elastic system fibers in the pubic symphysis of mice during pregnancy, partum and post-partum. Brazilian Journal of Morphology Science 2003; 20:85–92.
19. Ortega HH, Joazeiro PP, Muñoz-de-Toro MM, Luque EH, Montes GS. Differential distribution of the fibers of the collagenous and elastic systems and of glycosaminoglycans in the rat pubic joint. J Submicrosc Cytol Pathol 2001; 33:463–472.
20. Pinheiro MC, Joazeiro PP, Mora OA, Toledo OM. Ultrastructural and immunohistochemistry analysis of proteoglycans in mouse pubic symphysis. Cell Biol Int 2003; 27:647–655.
21. McDonald JK, Schwabe C. Relaxin induced elevations of cathepsin B and dipeptidyl peptidase I in the mouse pubic symphysis, with localization by fluorescence enzyme histochemistry. Ann N Y Acad Sci 1982; 380:178–186.
22. Rosa RG, Tarsitano CA, Hyslop S, Yamada AT, Toledo OM, Joazeiro PP. Temporal changes in matrix metalloproteinases, their inhibitors and cathepsins in mouse pubic symphysis during pregnancy and postpartum. Reprod Sci 2011; 18:963–977.
23. Weiss M, Nagelschmidt M, Struck H. Relaxin and collagen metabolism. Hormone Metab Res 1979; 11:408–410.
24. Stegmann H, Stalder K. Determination of hydroxyproline. Clin Chim Acta 1967; 18:267–273.
25. Akins ML, Luby-Phelps K, Bank RA, Mahendroo M. Cervical softening during pregnancy: regulated changes in collagen cross-linking and composition of matricellular proteins in the mouse. Biol Reprod 2011; 84:1053–1062.
26. Ruscheinsky M, De La Motte C, Mahendroo M. Hyaluronan and its binding proteins during cervical ripening and parturition: dynamic changes in size, distribution and temporal sequence. Matrix Biol 2008; 27:487–497.
27. Calabro A, Benavides M, Tammi M, Hascall VC, Midura RJ. Microanalysis of enzyme digests of hyaluronan and chondroitin/dermatan sulfate by fluorophore-assisted carbohydrate electrophoresis (FACE). Glycobiology 2000; 10:273–281.
28. Calabro A, Hascall VC, Midura RJ. Adaptation of FACE methodology for microanalysis of total hyaluronan and chondroitin sulfate composition from cartilage. Glycobiology 2000; 10:283–293.
29. Laborda J. 36B4 cDNA used as an estradiol-independent mRNA control is the cDNA for human acidic ribosomal phosphoprotein PO. Nucleic Acids Res 1991; 19:3998.
30. Samuel CS, Coghlan JP, Bateman JF. Effects of relaxin, pregnancy and parturition on collagen metabolism in the rat pubic symphysis. J Endocrinol 1998; 159:117–125.
31. Pinheiro MC, Mora OA, Caldini EG, Battlehner CN, Joazeiro PP, Toledo OM. Ultrastructural, immunohistochemistry and biochemical analysis of glycosaminoglycans and proteoglycans in the mouse pubic symphysis during pregnancy. Cell Biol Int 2005; 29:458–471.
32. Esko JD, Kimata K, Lindahl U. Proteoglycans and sulfated glycosaminoglycans. In: Varki A, Cummings RD, Esko JD, Freeze HH, Stanley P, Bertozzi CR, Hart GW, Etzler ME (eds.), Essentials of Glycobiology, 2nd ed. Cold Spring Harbor, NY: Cold Spring Harbor Laboratory Press; 2009.
33. Kyriakides TR, Zhu YH, Smith LT, Bain SD, Yang Z, Lin MT, Danielson KG, Iozzo RV, LaMarca M, McKinney CE, Ginns El, Bornstein P. Mice that lack thrombospondin 2 display connective tissue abnormalities that are associated with disordered collagen fibrillogenesis, an increased vascular density, and a bleeding diathesis. J Cell Biol 1998; 140:419–430.
34. Rentz TJ, Poobalarahi F, Bornstein P, Sage EH, Bradshaw AD. SPARC regulates processing of procollagen I and collagen fibrillogenesis in dermal fibroblasts. J Biol Chem 2007; 282:22062–22071.
35. Almond A. Hyaluronan. Cell Mol Life Sci 2007; 64:1591–1596.
36. Jiang D, Liang J, Noble PW. Hyaluronan as an immune regulator in human diseases. Physiol Rev 2011; 91:221–264.
37. Camenisch TD, Spicer AP, Brehm-Gibson T, Biesterfeldt J, Augustine ML, Calabro A Jr, Kubalak S, Klewer SE, McDonald JA. Disruption of hyaluronan synthase-2 abrogates normal cardiac morphogenesis and hyaluronan-mediated transformation of epithelium to mesenchyme. J Clin Invest 2000; 106:349–360.
38. Mjaatvedt CH, Yamamura H, Capehart AA, Turner D, Markwald RR. The Cspg2 gene, disrupted in the hdf mutant, is required for right cardiac chamber and endocardial cushion formation. Dev Biol 1998; 202:56–66.
39. Csoka AB, Frost GI, Stern R. The six hyaluronidase-like genes in the human and mouse genomes. Matrix Biol 2001; 20:499–508.
40. Sandy JD, Westling J, Kenagy RD, Iruela-Arispe ML, Verscharen C, Rodriguez-Mazaneque JC, Zimmermann DR, Lemire JM, Fischer JW, Wight TN, Clowes AW. Versican V1 proteolysis in human aorta in vivo occurs at the Glu441-Ala442 bond, a site that is cleaved by recombinant ADAMTS-1 and ADAMTS-4. J Biol Chem 2001; 276:13372–13378.
41. Russell DL, Doyle KM, Ochsner SA, Sandy JD, Richards JS. Processing and localization of ADAMTS-1 and proteolytic cleavage of versican during cumulus matrix expansion and ovulation. J Biol Chem 2003; 278:42330–42339.
42. Westling J, Gottschall PE, Thompson VP, Cockburn A, Perides G, Zimmermann DR, Sandy JD. ADAMTS4 (aggrecanase-1) cleaves human brain versican V2 at Glu405-Gln406 to generate glial hyaluronate binding protein. Biochem J 2004; 377:787–795.
43. Yao L, Cooke PS, Meling DD, Shanks RD, Jameson JL, Sherwood OD. The effect of relaxin on cell proliferation in mouse cervix requires estrogen receptor (alpha) binding to estrogen response elements in stromal cells. Endocrinology 2011; 151:2811–2818.
44. Yao L, Agoulnik AI, Cooke PS, Meling DD, Sherwood OD. Relaxin acts on stromal cells to promote epithelial and stromal proliferation and inhibit apoptosis in the mouse cervix and vagina. Endocrinology 2008; 149:2072–2079.
45. Straach KJ, Shelton JM, Richardson JA, Hascall VC, Mahendroo MS, Regulation of hyaluronan expression during cervical ripening. Glycobiology 2005; 15:55–65.
46. Timmons BC, Fairhurst AM, Mahendroo MS. Temporal changes in myeloid cells in the cervix during pregnancy and parturition. J Immunol 2009; 182:2700–2707.
47. Timmons BC, Mahendroo MS. Timing of neutrophil activation and expression of proinflammatory markers do not support a role for neutrophils in cervical ripening in the mouse. Biol Reprod 2006; 74:236–245.
48. Timmons B, Akins M, Mahendroo M. Cervical remodeling during pregnancy and parturition. Trends Endocrinol Metab 2010; 21:353–361.
49. Read CP, Word RA, Ruscheinsky M, Timmons BC, Mahendroo MS. Cervical remodeling during pregnancy and parturition: molecular characterization of the softening phase in mice. Reproduction 2007; 134:327–340.